

# Journal of Materials Chemistry A

Accepted Manuscript



This is an *Accepted Manuscript*, which has been through the Royal Society of Chemistry peer review process and has been accepted for publication.

*Accepted Manuscripts* are published online shortly after acceptance, before technical editing, formatting and proof reading. Using this free service, authors can make their results available to the community, in citable form, before we publish the edited article. We will replace this *Accepted Manuscript* with the edited and formatted *Advance Article* as soon as it is available.

You can find more information about *Accepted Manuscripts* in the [Information for Authors](#).

Please note that technical editing may introduce minor changes to the text and/or graphics, which may alter content. The journal's standard [Terms & Conditions](#) and the [Ethical guidelines](#) still apply. In no event shall the Royal Society of Chemistry be held responsible for any errors or omissions in this *Accepted Manuscript* or any consequences arising from the use of any information it contains.

Cite this: DOI: 10.1039/c0xx00000x

ARTICLE TYPE

www.rsc.org/xxxxxx

## An alternative anchoring methodology of organic sensitizers onto TiO<sub>2</sub> semiconductors for photoelectrochemical applications

Panagiotis Giannopoulos,<sup>a,b</sup> Archontoula Nikolakopoulou,<sup>b,c</sup> Aikaterini K. Andreopoulou,<sup>\*a,b</sup> Lamprini Sygellou,<sup>b</sup> Joannis K. Kallitsis,<sup>a,b</sup> and Panagiotis Lianos<sup>b,c</sup>

5

Received (in XXX, XXX) Xth XXXXXXXXXX 20XX, Accepted Xth XXXXXXXXXX 20XX

DOI: 10.1039/b000000x

In the present work, we investigated alternative ways of connecting purely organic dyes onto the surface of TiO<sub>2</sub> electrodes. For this purpose, perfluorophenyl  $\omega$ -end *rr*-poly(3-alkyl thiophene)s were synthesized, which can react with the hydroxyl groups of TiO<sub>2</sub> under mild alkaline conditions. Thus, stable non-hydrolysable Ti-O-C bonds are formed. Through this route, and after optimization of the reaction conditions, several poly(thiophene)-sensitized TiO<sub>2</sub> photoanodes were prepared and tested in Dye-sensitized solar cells. Moreover, a comparative study was performed for the dye/TiO<sub>2</sub> stability after water and alkaline solution treatment revealing the particular methodology's efficiency. The above sensitizers have also proven to be functional in photoelectrochemical cells employed for water splitting applications in the presence of alkaline electrolytes.

### Introduction

The conversion of solar light to usable forms of energy through low cost procedures, which is achieved by photovoltaic devices, is one of the most promising technological areas<sup>1,2</sup>. Although most solar light converters are made from silicon, their high cost of production has turned attention to organic solar cells, generally referred to as organic photovoltaics (OPV), where the device active layers mainly consist of organic materials<sup>3</sup>. A number of different OPV technologies have been developed so as to fulfill all requirements in efficiency, lifetime and cost. Among them, the most common structures are bulk heterojunction (BHJ)<sup>4</sup> and dye-sensitized solar cells (DSSCs)<sup>5,6</sup>.

DSSCs show higher efficiency and are thus ready for market penetration, owing to the great efforts that have been made since their discovery<sup>7</sup>. This has been achieved through optimization of cell's individual components without changing cell configuration. Starting from the inorganic semiconductor, which acts as electron acceptor and transporter, a lot of studies have been reported. For example, TiO<sub>2</sub><sup>8,9,10</sup>, ZnO<sup>11,12</sup> and SnO<sub>2</sub><sup>13,14,15</sup> have been tested, although TiO<sub>2</sub> is by far the most widely studied. This is due to the stability of titania nanoparticles, their satisfactory electronic properties the easiness of its synthesis and deposition and its relatively high-located conduction band, which provides a higher Fermi level and open-circuit voltage (V<sub>oc</sub>)<sup>16</sup>. Nowadays, studies mostly focus on the nanomorphology of the electrode from random formations to nanotubes or nanorods, that can provide

improved charge transport and hole conductor pore filling, which leads to better efficiencies.

Another crucial part in the DSSC technology is the photosensitizer, usually referred to as the Dye. The first dyes used by Grätzel's group were metal complexes, and in particular Ru(II) complexes<sup>7,17</sup>. The central metal ion is a crucial part of their functionality. After more than 20 years of intense research in the field of photosensitizers, Ru(II) complexes (typically with bipyridines and various substituents) are still being studied by researchers due to their satisfactory sensitization capacity<sup>18,19</sup>. On the other hand, ruthenium complexes have some drawbacks, such as their limited absorption in the near-infrared, the rareness of the central metal, which leads to high cost of the final device and its toxicity with the resulting environmental issues. Thus, a lot of alternative photosensitizers have been tested, some of them showing competitive results. For example, complexes with other metal ions, such as Cu<sup>20,21</sup>, Os<sup>22,23</sup> or Fe<sup>24,25</sup>, alternative ligands like porphyrins<sup>26,27</sup> and phthalocyanines<sup>28,29</sup>, and dyes based on organic molecules<sup>30,31,32,33</sup> (either monomers or polymers) have been tested. In particular, organic dyes exhibit many advantages over metallocomplexes, including easier synthetic routes, lower cost and scalability. They are also environmentally friendlier, although their cell efficiencies still remain lower compared to Ru(II) complexes. On the other hand, devices based on small molecules have shown excellent efficiencies for solid state DSSCs<sup>34</sup>, proving that they can be valid alternatives to ruthenium-based dyes.

Meanwhile, one of the most widely studied semiconducting

polymer acting as light absorber and electron donor-hole conductor is regioregular poly-3-hexylthiophene (P3HT) and its derivatives, employed both in BHJs' active layer or as sensitizer of TiO<sub>2</sub> in DSSCs. Especially, P3HT and its derivatives has been used in the past to sensitize TiO<sub>2</sub> nanoparticles by our group<sup>35</sup> and other works<sup>36,37</sup>. In the case of DSSCs, anchoring of polymers onto the TiO<sub>2</sub> surface is usually made by esteric bonds, after modification of the polymers with carboxylic groups, even though other groups such as, sulfonic and phosphonic, or even trialkoxysilane [Si(OR)<sub>3</sub>] acid have been used<sup>38,39,40</sup>. These bonds on the other hand may be strong, but are not stable in aqueous environments, therefore such polymer sensitized DSSCs are only limited to the use of pure organic electrolytes. To overcome this problem, different anchors, such as hydroxamate<sup>41,42</sup>, that proved to be more stable in aqueous environments, have been suggested.

In the present work, alternative ways of connecting purely organic dyes onto the surface of TiO<sub>2</sub> electrodes were investigated. More specifically, perfluorophenyl functionalized organic semiconducting materials (Organic-5F) were employed as dyes, since the pentafluorophenyl group can react with the hydroxyl groups of TiO<sub>2</sub> nanoparticles creating Ti-O-C bonds after removing the fluorine atom placed at para-position under mild alkaline conditions. This Ti-O-C bond, is more stable than the esteric bonds formed after typical reactions with carboxylic end-group molecules, since it is non-hydrolysable and therefore can overcome problems concerning aqueous environments. For this reason perfluorophenyl phenyl quinolines as small molecular dyes and perfluorophenyl  $\omega$ -end regioregular poly(3-alkyl thiophene)s were presently used for the functionalization of TiO<sub>2</sub> NPs. After optimization of the reaction conditions and thorough characterization of the Organic-5F-TiO<sub>2</sub> hybrids via various complementary techniques, several poly(thiophene)-sensitized TiO<sub>2</sub> photoanodes were prepared and evaluated in DSSCs. The stability of the dye/TiO<sub>2</sub> hybrids after water and alkaline solution treatment were tested in order to prove the methodology's efficiency. Thus, in addition to the application to DSSCs, these sensitizers have been proven functional in photoelectrochemical cells employed for water splitting applications in the presence of alkaline electrolytes.

## Experimental

### Materials

All solvents and reagents were purchased from Sigma Aldrich, Alfa Aesar or Acros Organics and were used without further purification unless otherwise stated. All reactions were carried out under argon atmosphere. 2,5-Dibromo-3-hexyl thiophene<sup>43</sup>, 6-phenyl-(2-perfluorophenyl)-4-phenyl-quinoline (Ph-5FQ)<sup>44</sup> were prepared according to literature procedures. Tetrahydrofuran (THF) was dried and distilled just before use over sodium wire in the presence of benzophenone. Commercial nanocrystalline titania Degussa P25 (specific surface area 50 m<sup>2</sup>/g) was used in all cell constructions and Millipore water was used in all experiments. SnO<sub>2</sub>:F transparent conductive electrodes (FTO, Resistance 8  $\Omega$ /square) were purchased from Pilkington. TiO<sub>2</sub> nanoparticles

prior to their reactions with the perfluorophenyl functionalized moieties, were calcined at 400°C for 3-4 hr to remove all hydrogen-bonded water molecules<sup>45</sup>.

### Characterization methods

<sup>1</sup>H, and <sup>19</sup>F, NMR spectra were recorded on Bruker Advance DPX 400.13, 100.6 and 376.5 MHz spectrometers, respectively, with CDCl<sub>3</sub> as solvent containing TMS as internal standard.

Thermogravimetric analysis (TGA) was carried out on 8 mg samples contained in alumina crucibles in a Labsys TM TG apparatus of Setaram under nitrogen and at a heating rate of 10 °C min<sup>-1</sup>. UV-Vis diffuse reflectance spectra (DRS) of the *rr*-P3HT-5F-TiO<sub>2</sub> photoanodes on glass substrate, were measured with a Cary 3 spectrophotometer equipped with an integration sphere in the range of 200 nm-800nm. Pure TiO<sub>2</sub> substrate was also measured for comparison. IR spectra were recorded on a Perkin-Elmer 16PC FTIR spectrometer and on an ALPHA-P diamond ATR spectrometer of Bruker Optics GmbH. UV-Vis spectra were recorded using a Hitachi U-1800 spectrophotometer. Photoluminescence (PL) spectra were recorded using a Perkin-Elmer LS45 luminescence spectrometer, after excitation at the UV-Vis absorption maxima. Scanning electron microscopy (SEM) pictures were taken using a LEO Supra 35VP FEG-SEM microscope. Transmission electron microscopy (TEM) measurements were performed on a JEOL JEM2100 operating at 200 kV. Sample preparation for TEM examination involved the preparation of dilute suspensions of the samples in o-DCB/EtOH or absolute EtOH. A drop of the solution was placed on 3 mm carbon coated copper grids (Electron Microscopy Sciences) and the samples were dried in air for 2 days. The surface analysis studies were performed in a UHV chamber (P<10<sup>-9</sup> mbar) equipped with a SPECS LHS-10 hemispherical electron analyzer. XPS measurements were carried out at room temperature using unmonochromatized AlK $\alpha$  radiation under conditions optimized for maximum signal (constant  $\Delta E$  mode with pass energy of 97 eV giving a full width at half maximum (FWHM) of 1.7 eV for the Au 4f<sub>7/2</sub> peak). The analyzed area was an ellipse with dimensions 2.5x4.5mm<sup>2</sup>. The XPS core level spectra were analyzed using a fitting routine, which can decompose each spectrum into individual mixed Gaussian-Lorentzian peaks after a Shirley background subtraction. The samples were dissolved in DCB and spin coated on silicon substrate. Before deposition the silicon substrates were subjected to oxygen plasma treatment (rf=10.5W, 5min) in order to remove carbon contamination and to improve surface wetting and hence the coatings homogeneity. X-Ray Diffraction (XRD) measurements were conducted using a Bruker D8 Advance Cu K $\alpha$  radiation ( $\lambda = 0.15418$  nm). The XRD measurements were carried out in the  $2\theta$  angle with the range of 20–90°.

DSSC characterization was made by illumination of the samples with a PECCELL PEC-L01 Solar Simulator set at 100 mW/cm<sup>2</sup>. IV characteristics were recorded under ambient conditions with a Keithley 2601 source meter. In the case of photoelectrochemical water splitting, current voltage curves were recorded by illumination with the same solar simulation and with the help of an Autolab PGSTAT128N potentiostat.

The latter were traced in a two-electrode configuration (i.e. without a reference electrode) at  $5 \text{ mV}\cdot\text{s}^{-1}$ .

### Synthetic procedures

#### Synthesis of 2-Perfluorophenyl terminated regioregular poly(3-hexylthiophene) (P3HT-5F)

*Synthesis of rr-P3HT*<sup>43</sup>  
2,5-Dibromo-3-hexyl-thiophene (1.02g, 3.126mmol, 1eq) was dissolved in 15mL of distilled THF in a round bottom flask equipped with a stir bar and a reflux condenser, under inert atmosphere. 1.04mL of MeMgCl (3M in diethyl ether, 3.126mmol, 1eq) was added via syringe and the reaction was heated at reflux for 2 hours. After cooling at room temperature, 33.9mg of Ni(dppp)Cl<sub>2</sub> (0.0625mmol, 0.02eq) was added, and the reaction mixture was stirred at RT overnight. Then the mixture was precipitated in MeOH, filtrated and purified by Soxhlet extraction using subsequent solvents MeOH, *n*-hexane and CHCl<sub>3</sub>. The *n*-hexane and CHCl<sub>3</sub> fraction were evaporated and dried under vacuum overnight. The *n*-hexane fraction was used further for  $\omega$ -end group modification with perfluorophenyl groups.

#### *Synthesis of rr-P3HT-5F*

*rr*-P3HT *n*-hexane fraction (105mg, 0.25mmol, 1eq), pentafluorophenyl boronic acid (65mg, 0.3mmol, 1.2eq) and Pd(PPh<sub>3</sub>)<sub>4</sub> (13.3 mg, 0.012mmol, 0.04eq) were dissolved in 20mL of degassed toluene and to that solution were then added 0.8mL of a Na<sub>2</sub>CO<sub>3</sub> 2M solution (6eq). The solution was refluxed for 48h. After cooling to RT, the catalyst was removed by filtration. The solvent was evaporated under vacuum and the crude mixture was stirred in MeOH in order to remove impurities. The pure product *rr*-P3HT-5F was obtained by filtration and drying under vacuum overnight.

#### Preparation of phenyl-perfluorophenyl-phenylquinoline-TiO<sub>2</sub> (Ph5FQ-TiO<sub>2</sub>) hybrid NPs

*A representative example corresponding to entry 5 of Table 1 is described below. Analogues conditions were used in all other cases.*

To a degassed round-bottom flask equipped with a reflux condenser and a magnetic stirrer under an argon atmosphere 30mg (0.067mmol, 1eq) of phenyl-perfluorophenyl-phenylquinoline and 37mg (0.268mmol, 4eq) of K<sub>2</sub>CO<sub>3</sub> were dispersed in 40mL of acetone. TiO<sub>2</sub> nanoparticles (100mg), that were first thermally treated for 3-4hr at 400°C and stored in a desiccator, were then added in the reaction mixture. The mixture was heated at reflux for 48h. After cooling at room temperature, the mixture was filtrated and washed with acetone, water and THF to remove the salts and the unreacted quinoline molecules, until the filtrate was colourless and then was dried in a vacuum oven overnight.

#### Preparation of rr-P3HT-5F-TiO<sub>2</sub> hybrid NPs

A mixture of *rr*-P3HT-5F (0.067mmol), TiO<sub>2</sub> powder (50mg) and K<sub>2</sub>CO<sub>3</sub> 37mg(0.268mmol) in acetone was heated under Ar at reflux for 48h. After cooling at room temperature, the mixture was filtrated and washed with THF and water to remove unreacted polymer and salts. The powder was dispersed afterwards in THF, centrifuged at 13000rpm and finally the supernatant was removed. This procedure was repeated until

the supernatant was colourless. The crude product (22mg) was dried under vacuum oven overnight.

#### Preparation of the blend rr-P3HT-5F/TiO<sub>2</sub>

TiO<sub>2</sub> powder (43.5mg) and *rr*-P3HT (*n*-hexane fraction) (6.5mg) were dissolved in 20mL acetone. The mixture was sonicated for 20min then it was stirred at 60°C for 48hr. Finally, the mixture was purified as described above for the *rr*-P3HT-5F-TiO<sub>2</sub> hybrid NPs.

#### Deposition of nanoparticulate titania films on FTO electrodes

Photoanode electrodes were made by depositing a nanocrystalline titania (nc-TiO<sub>2</sub>) film on an FTO electrode by a standard procedure employed in our previous publications<sup>46</sup>. A FTO transparent electrode was cut in the appropriate dimensions and was carefully cleaned first with soap and then by sonication in isopropanol, water and acetone. A thin layer of compact titania was first sprayed over the FTO electrode using 0.2 mol L<sup>-1</sup> diisopropoxytitanium bis(acetylacetonate) solution in ethanol and then it was calcined at 500 °C. On this thin bottom layer, a titania paste made of P25 nanoparticles was applied by doctor blading. The film was calcined again up to 550 °C at a rate of 20 °C/min. The final thickness of the film, as measured by SEM, was approximately 10 μm. Then, the film was treated with a 0.04 mol L<sup>-1</sup> aqueous solution of TiCl<sub>4</sub> for 30 min at 70 °C, followed by calcination up to 500 °C. The active geometrical area of the film was 1 cm<sup>2</sup> (1 cm x 1 cm) in all studied cases.

#### Preparation of rr-P3HT-5F-TiO<sub>2</sub> sensitized photoanodes

*A representative example corresponding to entry 6 of Table 2 is described below. Analogue conditions were used in all other cases.*

A TiO<sub>2</sub> photoanode was placed in a mixture of acetone (30mL), *rr*-P3HT-5F (0.067mmol) and K<sub>2</sub>CO<sub>3</sub> (0.268mmol). The system was heated at reflux under Ar for 48h. After cooling at room temperature, the photoanode was taken out of the solution and was thoroughly washed in THF, water and acetone. Finally, it was dried under vacuum overnight.

#### Construction of devices

DSSCs were made by a standard procedure<sup>46,47</sup> where an electrolyte containing the I<sub>3</sub>/I<sup>-</sup> redox couple was sandwiched between a sensitized as above photoanode electrode and a counter electrode. The counter electrode was also a FTO glass functionalized with Pt electrocatalyst. Pt nanoparticles were deposited by twice spin coating a solution of 0.02 mol L<sup>-1</sup> chloroplatinic acid hexahydrate in isopropanol and subsequent calcination at 550 °C. The electrolyte was based on a Ureasil precursor, same as for the reported synthetic procedures:<sup>47,48</sup> 1.2 g of sulfolane and 1.2 g of 3-methoxypropionitrile were mixed under stirring with 0.7 g of the above Ureasil precursor, 0.35 mL of acetic acid (AcOH), 0.12 g LiI and 0.12 g 1-methyl-3-propylimidazolium iodide. When the solution was clear, we added 0.06 g I<sub>2</sub>. Thus, the molar ratio of I<sup>-</sup> to I<sub>2</sub> was approximately 6:1. Finally, we added about 0.5 mol.L<sup>-1</sup> tert-butylpyridine and 0.1 mol.L<sup>-1</sup> guanidinium thiocyanate, which are known to raise the open-circuit voltage and the short-circuit

current in DSSCs, respectively. The solution was stirred for several hours before application. During this period, a slow solvolysis took place developing silica bonds between precursor chains and leading to condensation and gel formation.<sup>47,48</sup> One drop of this mature gel was placed on the photoanode electrode and the counter electrode was placed on the top and pressed by hand. The gel acts as an adhesive resin and holds the two electrodes together. No sealing was necessary. After a few hours, the gel dries and the cell is ready for characterization.

Photoelectrochemical studies using alkaline electrolyte were performed on a cell made of Plexiglas, supporting on opposite sides and parallel to each other the photoanode and counter electrode. The distance between them was 5 mm. The space between the electrodes was filled with aqueous 0.5 M NaOH. The photoanode played the role of cell window while the counter electrode was made of carbon cloth and was exposed to the ambient atmosphere. The counter electrode carried a mixture of Pt with carbon black as electrocatalyst at the same time providing a hydrophobic layer that prevented electrolyte leak.<sup>49</sup> The active size of the photoanode electrode was 1 cm<sup>2</sup> (1 cm x 1cm) and of the counter electrode 2.25 cm<sup>2</sup> (1.5 cm x 1.5 cm).

## Results and Discussion

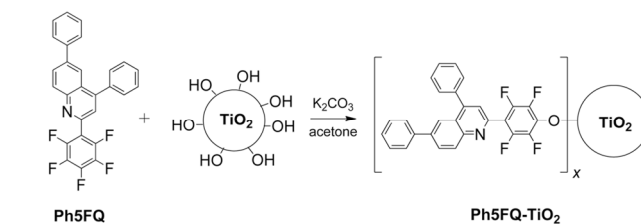
Current trends in TiO<sub>2</sub> sensitization with dyes, either metal complexes or purely organic molecules, are realized mostly through ester bond formation between the hydroxyl groups of TiO<sub>2</sub> and carboxylic groups present in the dyes. These ester bonds, however, are readily hydrolysed under alkaline or acidic conditions, and for that reason such sensitized TiO<sub>2</sub> anodes are strictly protected from humidity and carefully kept and further used under inert atmospheres. These facts prompt us to investigate alternative ways of connecting purely organic dyes onto TiO<sub>2</sub> electrodes. The employment of purely organic dyes aimed also to circumvent additional drawbacks of typical ruthenium ion metal complexes such as availability, toxicity and scalability as clearly stated above.

### Sensitization of TiO<sub>2</sub> with Ph-5FQ

Perfluorophenyl groups are stable multi-purpose functionalities<sup>50</sup> that can be, for example, transformed to azides<sup>44</sup> or react with hydroxyl groups. Thus, we first studied a small molecular sensitizer carrying perfluorophenyl units in order to investigate their ability to react under alkaline conditions with the hydroxyl groups of commercial TiO<sub>2</sub> nanoparticles (Degussa P25), which is commonly used in DSSCs. This reaction is similar to the etherification reaction of hydroxyl compounds with perfluorophenyl functionalities. As shown in **Scheme 1** and **Table 1**, 6-phenyl-(2-perfluorophenyl)-4-phenyl-quinoline (Ph-5FQ) was used for the initial screening and optimization of the reaction conditions.

Different conditions were tested (**Table 1**) by varying reactants ratio, solvent and concentration of the reaction solution, temperature and time. Moreover, as given in entries 4 and 5 of **Table 1**, TiO<sub>2</sub> was previously thermally treated at 400°C for about 3 hours. This thermal treatment (also referred to as activation) removes hydrogen-bonded water molecules

thus, the number of the free surface hydroxyl groups and their activity is enhanced.<sup>45</sup> As base for achieving the required alkaline conditions, potassium hydroxide (KOH) and potassium carbonate (K<sub>2</sub>CO<sub>3</sub>) were employed while the solvents tested were acetone and DMF. In all cases filtration and centrifugation were employed to collect the hybrid material Ph5FQ-TiO<sub>2</sub> after completion of the reaction. Then they were copiously washed using acetone or DMF, water and again acetone or DMF, in order to remove unreacted Ph5FQ and base as well as the produced KF salt. Optimal conditions were found by the above experiments and were based on the use of previously activated TiO<sub>2</sub> with K<sub>2</sub>CO<sub>3</sub> as base in acetone for 48hr.



**Scheme 1:** Reaction of phenyl-perfluorophenyl-phenylquinoline with TiO<sub>2</sub> NPs producing organic-inorganic hybrids, Ph5FQ-TiO<sub>2</sub>.

**Table 1:** Reaction conditions and product quantities for the preparation of Ph-5FQ-TiO<sub>2</sub> hybrid NPs.

| a/a | TiO <sub>2</sub> (mg) | Ph-5FQ (mg) | Base / Solvent                          | Time (hr) | Ph5FQ-TiO <sub>2</sub> NPs (mg) |
|-----|-----------------------|-------------|---|-----------|---------------------------------|
| 1   | 30 <sup>a</sup>       | 30          | KOH/DMF                                 | 24        | 2                               |
| 2   | 30 <sup>a</sup>       | 30          | K <sub>2</sub> CO <sub>3</sub> /DMF     | 24        | 2                               |
| 3   | 30 <sup>a</sup>       | 30          | K <sub>2</sub> CO <sub>3</sub> /acetone | 48        | 5                               |
| 4   | 30 <sup>b</sup>       | 30          | K <sub>2</sub> CO <sub>3</sub> /acetone | 48        | 15                              |
| 5   | 90 <sup>b</sup>       | 30          | K <sub>2</sub> CO <sub>3</sub> /acetone | 48        | 45                              |

<sup>a</sup>) Degussa P25 without previous thermal treatment

<sup>b</sup>) Degussa P25 thermally treated at 400°C for 3 hr and stored in a desiccator

**Figure 1** presents the thermogravimetric analysis and ATR spectra of the hybrid material Ph5FQ-TiO<sub>2</sub> entry 5 of **Table 1**, in comparison to the net components. The successful binding of the molecules into the TiO<sub>2</sub> substrate was verified by TG analysis as shown in **Figure 1a**. The neat TiO<sub>2</sub> after thermal treating showed no significant weight loss between 50°C and 800°C, while perfluorophenyl-phenyl phenylquinoline (Ph-5FQ) was completely degraded around 400 °C. In the TGA analysis of the Ph-5FQ-TiO<sub>2</sub> hybrid material, the maximum degradation temperature was around 600°C and the weight loss was 55%. The higher stability of the hybrid sample (according to both temperature and weight loss) indicates the successful

formation of Ti-O-C bonds on the TiO<sub>2</sub> surface.

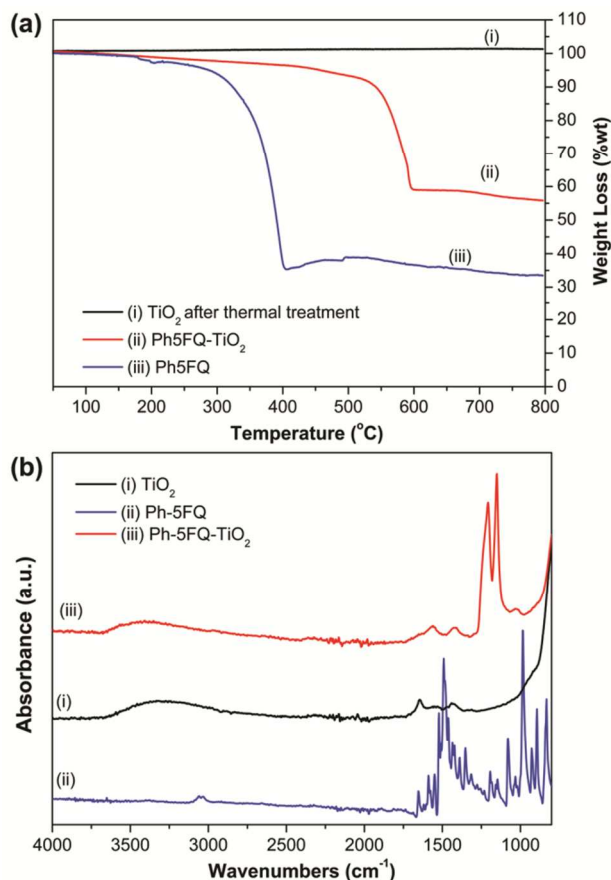
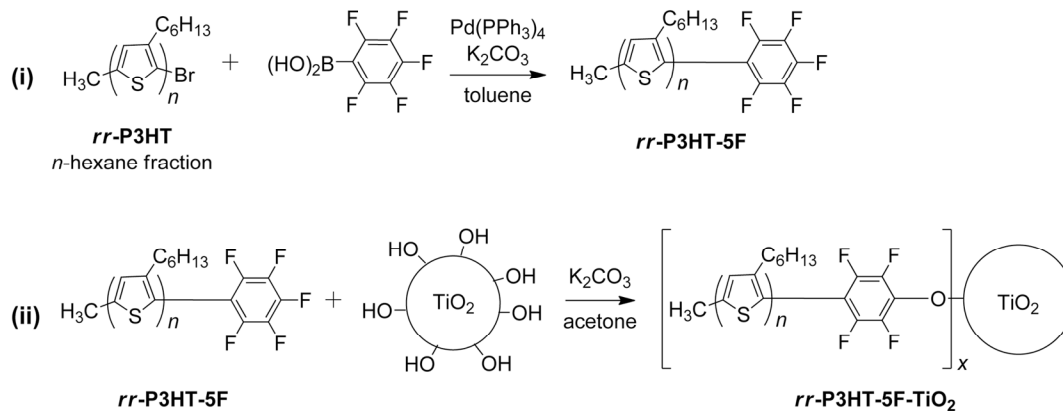


**Figure 1:** (a) TGA and (b) ATR spectra of TiO<sub>2</sub>, Ph5FQ and Ph5FQ-TiO<sub>2</sub> hybrid NPs.

The success of the reaction was further confirmed by ATR spectroscopy as shown in **Figure 1b**, in which it is clearly shown that besides the absorption bands of pure TiO<sub>2</sub><sup>51</sup>, located at 1600 cm<sup>-1</sup>, the spectrum of the hybrid product presents additional absorption bands at 1300-1100 cm<sup>-1</sup> due to attachment of phenyl-pentafluorophenyl-phenylquinoline. More specifically, the band centered at 1150 cm<sup>-1</sup> proves the formation of the Ti-O-C bond in the hybrid product<sup>52,53,54</sup>, whereas the pick due to the C-F stretching vibration, which is



**Scheme 2:** (i) synthesis of perfluorophenyl  $\omega$ -end functional *rr*-P3HT (*rr*-P3HT-5F) and (ii) its use for the preparation of *rr*-P3HT-5F-TiO<sub>2</sub> hybrid NPs.

usually coupled with other vibrations and thus is very difficult to be assigned, is slightly displaced in comparison with the starting molecule's spectra, around 1250 cm<sup>-1</sup>.<sup>55</sup>

### Sensitization of TiO<sub>2</sub> with *rr*-P3HT-5F

After the above encouraging results of successful connection of perfluorophenyl functionalized quinoline onto the hydroxyl decorated TiO<sub>2</sub> NPs, we proceeded with the development and use of the more efficient and highly absorbing regioregular poly(3-alkyl thiophene) bearing perfluorophenyl end-functionalities.

2,5-Dibromo-3-hexyl-thiophene was polymerized under typical GRIM polymerization in freshly distilled THF using MeMgCl as the Grignard reagent and NiCl<sub>2</sub>(dppp) as catalyst.<sup>43</sup> The crude polymer obtained after precipitation in methanol was then purified and fractionated via Soxhlet extraction using methanol, *n*-hexane and finally chloroform. For the purpose of this work we used only the *n*-hexane extract that provided a polymeric fraction with smaller molecular weights, (M<sub>n</sub> = 1050, M<sub>w</sub> = 1200, corresponding to a number of repeating units of approximately *n*=6). Analogous was the calculated molecular characteristics from <sup>1</sup>H NMR spectroscopy were end group analysis gave an *n*=5. The reason of choosing small molecular weight *rr*-P3HT as sensitizer was to enhance its incorporation in the TiO<sub>2</sub> NPs mesoporous structure and to avoid total coverage of the TiO<sub>2</sub> layer that could lead to its insulation and loss of its contact to the electrolyte.

The GRIM method is considered as a “living” polymerization reaction since at the  $\omega$ -polymeric chain end an active bromine group is present. This can be further employed for functionalizing the polymeric chains with active groups such as vinyl, hydroxyphenyl, etc, under palladium mediated Suzuki coupling of the bromine with aromatic boronic acids.<sup>56</sup> In our case we used the perfluorophenyl boronic acid in order to incorporate the desired perfluorophenyl functionalities onto the *rr*-poly(3-hexyl thiophene) chains ends, **Scheme 2i**. The successful introduction of the perfluorophenyl chain end-functionalities was proven by <sup>19</sup>F NMR spectroscopy as shown in **Figure 2**, where three peaks owing to the three different species of attached fluorines were detected.

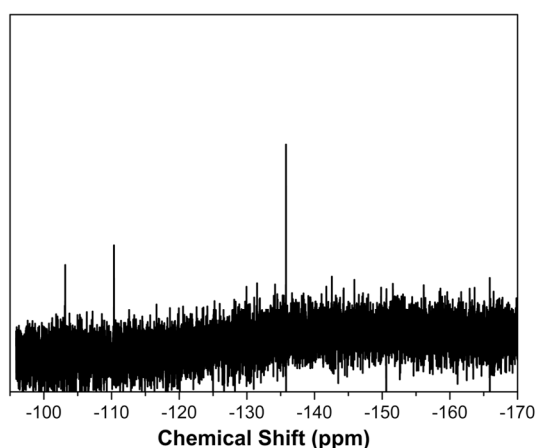


Figure 2:  $^{19}\text{F}$  NMR spectrum of *rr*-P3HT-5F in  $\text{CDCl}_3$ .

Using analogues to the above described conditions for the preparation of **Ph5FQ-TiO<sub>2</sub>** hybrid NPs, we proceeded with the development of the desired ***rr*-P3HT-5F-TiO<sub>2</sub>** hybrid NPs, **Scheme 2ii**. Also in this case thermally treated TiO<sub>2</sub> at 400°C for 3hr was used and we employed extensive washing and centrifugation steps for the purification of the prepared hybrids with water and THF, to remove all traces of salts and unreacted *rr*-P3HT-5F from the final samples. Initial characterization was performed via TGA and IR as shown in **Figure 3**.

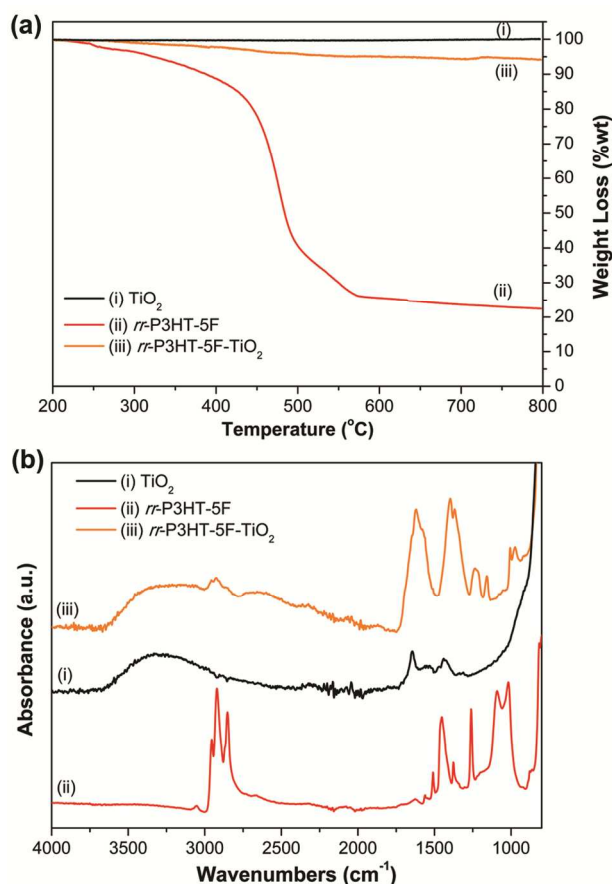


Figure 3: (a) TGA and (b) ATR spectra of  $\text{TiO}_2$ , *rr*-P3HT-5F and *rr*-P3HT-5F-TiO<sub>2</sub> hybrid NPs.

The attachment of the *rr*-P3HT moieties onto the TiO<sub>2</sub> NPs is proven by the increased thermal stability of the hybrid materials versus the pure polymeric precursor (**Figure 3a**). From the TGA diagrams, a 13% functionalization of TiO<sub>2</sub> NPs with *rr*-P3HT-5F can be calculated. Moreover, there is a clear coexistence of the P3HT and of the TiO<sub>2</sub> IR peaks as evident in **Figure 3b**, which is accompanied by alterations of the *rr*-P3HT-5F peaks below 1600  $\text{cm}^{-1}$  due to the Ti-O-C bond formation  $\text{C}_{\text{Ar}}\text{-F-O-TiO}_2$ , similar to the above described behaviour of the Ph5FQ-TiO<sub>2</sub> hybrid NPs.

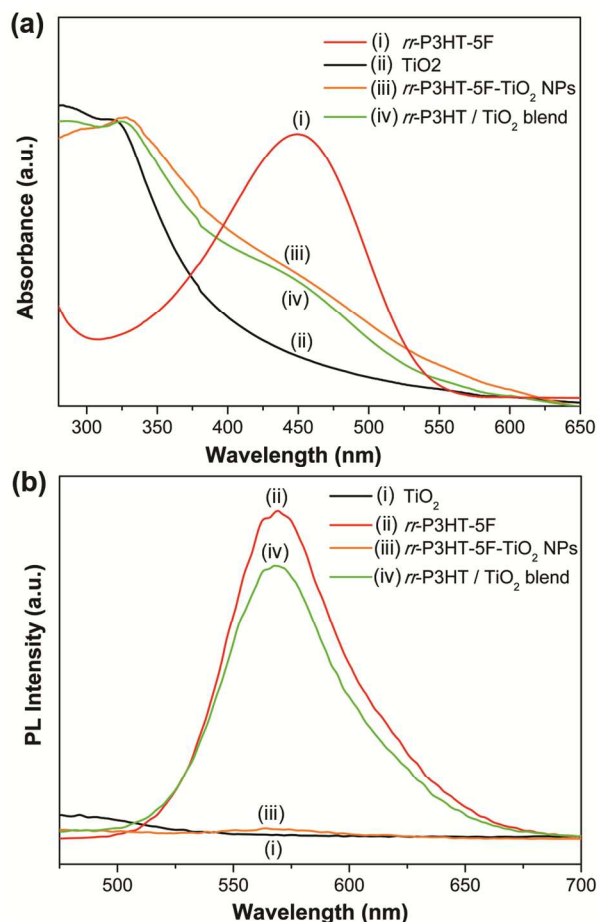
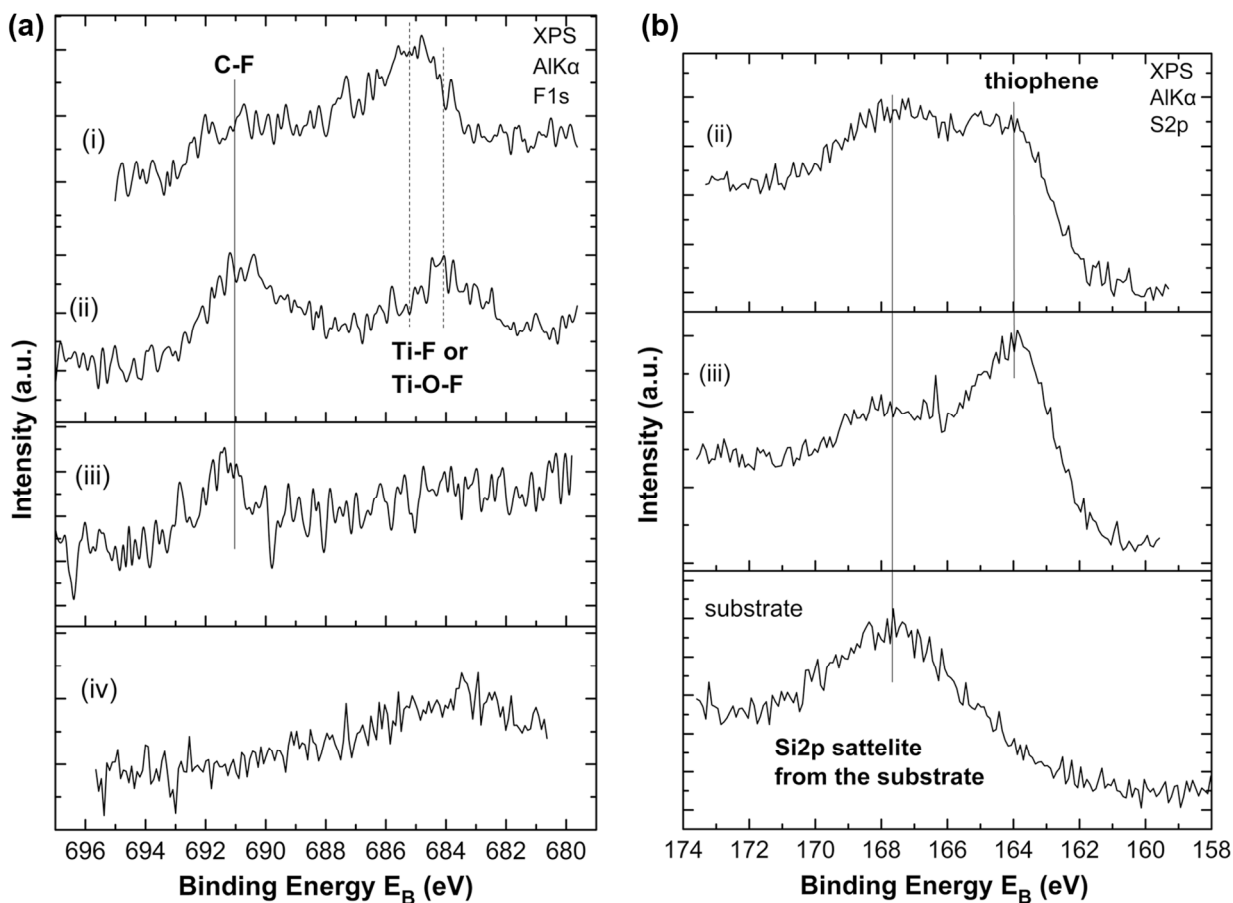


Figure 4: (a) UV-Vis and (b) PL spectra of the starting materials  $\text{TiO}_2$  and *rr*-P3HT-5F, of the final *rr*-P3HT-5F-TiO<sub>2</sub> hybrid NPs and of the *rr*-P3HT-5F/TiO<sub>2</sub> physical blend all in  $\text{CHCl}_3$  solutions. The PL spectra were recorded after excitation at the P3HT's absorption maximum 450nm.

The UV-Vis and PL spectra of the ***rr*-P3HT-5F-TiO<sub>2</sub>** hybrid NPs compared to the initial materials are given in **Figure 4a** and **4b**, respectively. In order to clarify differences in the optical properties of the hybridized TiO<sub>2</sub> NPs, at which P3HT has been bonded onto TiO<sub>2</sub> when compared to the initial TiO<sub>2</sub> powder, we prepared a blend of *rr*-P3HT (*n*-hexane fraction) with TiO<sub>2</sub> (***rr*-P3HT-5F/TiO<sub>2</sub>**) using the same conditions as for the *rr*-P3HT-5F-TiO<sub>2</sub> NPs. From the TGA data of *rr*-P3HT-5F-TiO<sub>2</sub> hybrid NPs (**Figure 3a**), it was calculated that the hybrid molecules consist of 87% TiO<sub>2</sub> nanoparticles and 13% *rr*-P3HT-5F (w/w), so the composition of the blend was kept the same. In **Figure 4a** the *rr*-P3HT-5F-TiO<sub>2</sub> NPs and of course

the blend *rr*-P3HT/TiO<sub>2</sub> present a shoulder in their absorption spectra where the poly(thiophene) absorbs, around 450nm. On the contrary the photoluminescence behaviour of the *rr*-P3HT-5F-TiO<sub>2</sub> NPs is drastically different compared to the blend *rr*-P3HT/TiO<sub>2</sub> as shown in **Figure 4b**, where the PL spectra of the initial materials, of the blend and of the final hybrid NPs are compared. In particular a photoluminescence quenching was detected for the hybrid *rr*-P3HT-5F-TiO<sub>2</sub> NPs after excitation

at the absorption maximum of *rr*-P3HT. The blend *rr*-P3HT/TiO<sub>2</sub> presented only a negligible reduction of its photoluminescence. This point strongly proves the covalent attachment of the *rr*-P3HT-5F moieties onto the TiO<sub>2</sub> NPs allowing the efficient electronic interactions between the two species, whereas a simple blend of the net components is simply insufficient.



**Figure 5.** (a) F1s XPS core level spectra of (i) Ph5FQ-TiO<sub>2</sub> NPs, (ii) *rr*-P3HT-5F-TiO<sub>2</sub> NPs, (iii) *rr*-P3HT-5F/TiO<sub>2</sub> blend and (iv) TiO<sub>2</sub> in powder form; and (b) S2p XPS core level spectra for the (substrate) plasma-treated Si, (ii) *rr*-P3HT-5F-TiO<sub>2</sub> NPs and (iii) *rr*-P3HT-5F/TiO<sub>2</sub> blend films.

XPS measurements were also conducted in order to further investigate and prove the direct and covalent attachment of the semiconducting *rr*-P3HT-5F chains onto TiO<sub>2</sub>. **Figure 5a** shows the F1s core level peak of the samples *rr*-P3HT-5F-TiO<sub>2</sub> NPs, of Ph5FQ-TiO<sub>2</sub> NPs entry 5 of **Table 1** and of *rr*-P3HT-5F/TiO<sub>2</sub> blend. A pure TiO<sub>2</sub> powder was also measured for comparison. Based on the binding energy (BE) values of a strong photoelectron peak, information about the chemical state for each element can be obtained. The TiO<sub>2</sub> sample showed that there is no fluorine whereas in the other three samples F1s peaks are observed. For the blend sample the spectrum shows only one peak at ~691eV assigned to covalent C-F bonds indicating that there is no interaction between TiO<sub>2</sub> and *rr*-P3HT-5F. For the Ph5FQ-TiO<sub>2</sub> NPs and *rr*-P3HT-5F-TiO<sub>2</sub> NPs the spectra consist of two components. The first at high binding energy originating from covalent C-F bonds and the second at low binding energy 684.2-685.2eV This peak which

is commonly observed in surface-fluorinated TiO<sub>2</sub> systems originating from fluorine atoms in terminal Ti-F or Ti-O-F bonds on the TiO<sub>2</sub> crystal surface.<sup>57</sup> **Figure 5b** shows the S2p spectra for the *rr*-P3HT-5F/TiO<sub>2</sub> blend and the *rr*-P3HT-5F-TiO<sub>2</sub> NPs sample. A spectrum from a clean Si substrate was added to evaluate the contribution of the substrate to the spectra's background. The S2p BE centered at 164.0eV is assigned to thiophene<sup>58</sup>, while the contribution at about 168 eV originated from the substrate (Si2p satellite feature). The binding energy of C1s and Ti2p core level peaks (not shown) are in 285.1eV assigned to C in thiophene and at 458.6eV assigned to TiO<sub>2</sub>. From the above results it is obvious that Ti-O-F bonds are present both in Ph5FQ-TiO<sub>2</sub> NPs and *rr*-P3HT-5F-TiO<sub>2</sub> NPs samples which is a clear indication that the semiconducting species carrying perfluorophenyl functionalities have been attached onto the TiO<sub>2</sub> NPs.

SEM analysis of the hybrid material was performed as



shown in **Figure 6** in comparison to the net  $\text{TiO}_2$  powder. In **Figure 6a** the SEM image of  $\text{TiO}_2$  shows the expected sharp NPs of well resolved edges whereas in **Figure 6b** a surrounding film around the  $\text{TiO}_2$  NPs is clearly seen due to the attached P3HT polymeric chains. This is more clearly observed in the TEM images of the pure  $\text{TiO}_2$  powder, **Figure 7a** versus the functionalized hybrid *rr*-P3HT-5F- $\text{TiO}_2$  NPs, **Figure 7b**.

In the XRD powder patterns of the *rr*-P3HT-5F- $\text{TiO}_2$  hybrid NPs **Figure 8**, only  $\text{TiO}_2$  reflections were detected probably due to the low P3HT content in the sample (~ 13% as calculated by TGA) that was not sufficient to provide crystalline domains. Moreover, the preservation of the anatase form of  $\text{TiO}_2$  in the final hybrid NPs is demonstrated by the XRD analysis, which is favourable for DSSCs applications<sup>16</sup>, providing another advantage of the herein presented methodology.

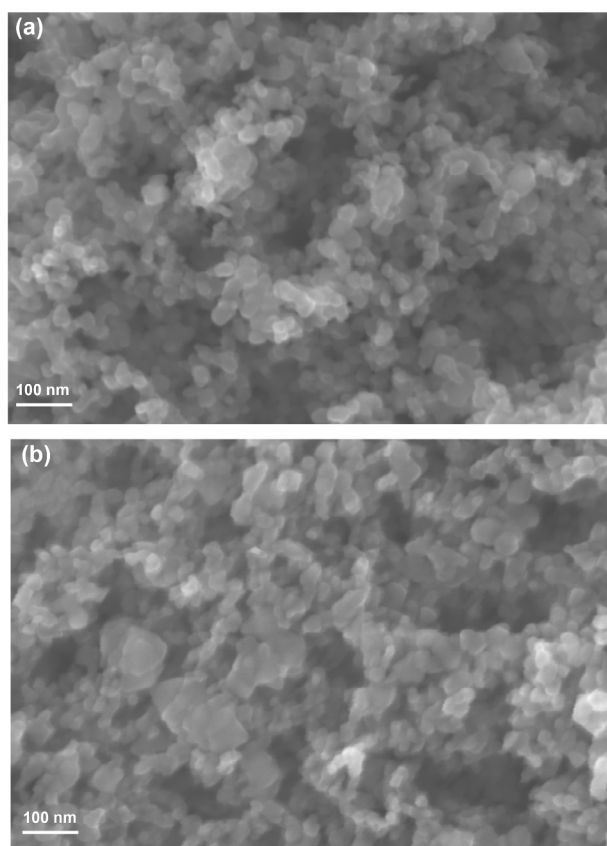
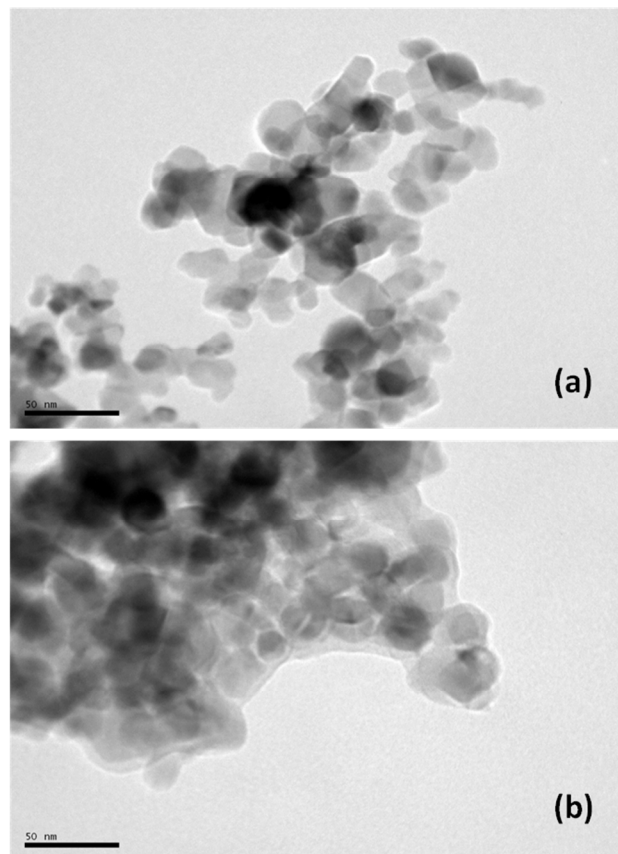


**Figure 6:** SEM images (a) of  $\text{TiO}_2$  NPs in powder form thermally treated at  $400^\circ\text{C}$  for 3hr and (b) of the *rr*-P3HT-5F- $\text{TiO}_2$  hybrid NPs in powder form.

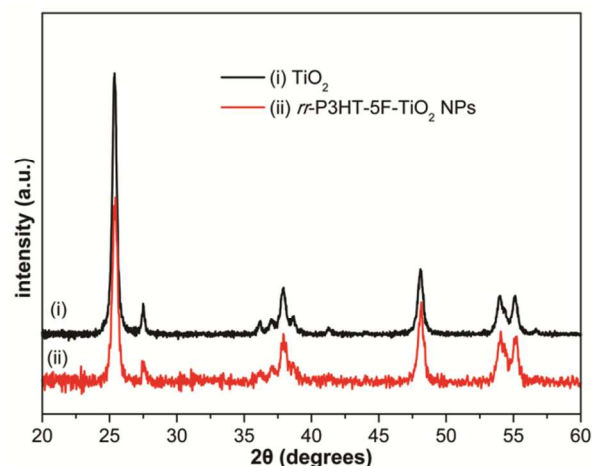
#### *rr*-P3HT-5F- $\text{TiO}_2$ sensitized photoanodes

For the preparation of the *rr*-P3HT-5F sensitized  $\text{TiO}_2$  photoanode electrodes, the deposited nanoparticulate titania films on FTO electrodes were immersed into solutions of *rr*-P3HT-5F in the presence of  $\text{K}_2\text{CO}_3$ . **Table 2** provides several conditions exploited together with the images of the respective sensitized photoanodes. After further optimization of the reaction conditions entries 4-7 of **Table 2**, intense red coloured photoanodes were obtained. In all cases the images of **Table 2** were taken after thorough washing of the sensitized photoanode

with THF, water and finally acetone in order to remove all traces of unreacted materials or produced salts.



**Figure 7:** TEM images (a) of  $\text{TiO}_2$  NPs in powder form thermally treated at  $400^\circ\text{C}$  for 3hr and (b) of the *rr*-P3HT-5F- $\text{TiO}_2$  hybrid NPs in powder form.

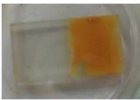








**Figure 8:** XRD patterns of (i)  $\text{TiO}_2$  NPs in powder form thermally treated at  $400^\circ\text{C}$  for 3hr and (ii) of the *rr*-P3HT-5F- $\text{TiO}_2$  hybrid NPs.

As already explained, the main driving force of this work was the development of a novel methodology for the production of efficient polymeric dye sensitized  $\text{TiO}_2$  NPs and their respective photoanodes, of excellent stability under air and humidity. To prove the stability of the prepared *rr*-P3HT-5F- $\text{TiO}_2$  photoanodes we immersed the sample (entry 7 of **Table 2**) subsequently in THF, water and finally in aqueous

NaOH 2M solution for 30 minutes and recorded its UV-Vis diffuse reflectance spectra inbetween subsequent immersions as shown in **Figure 9**. It is evident that the colouring of the sample remained almost intact (**Figure 9b**). The UV-Vis diffuse reflectance spectra (**Figure 9a**), which have been normalized at the 310 nm peak owing to TiO<sub>2</sub>, show some small alterations in the absorptivity of the samples. The red curve corresponds to the initial sample immediately after its removal from the reaction mixture. After thorough washing with THF all physisorbed P3HT onto the TiO<sub>2</sub> surface is removed (blue curve), which as expected shows a reduction of the P3HT content from the initial untreated photoanode. Thereafter, immersion in H<sub>2</sub>O (pink curve) and in aqueous NaOH 2M (green curve) presented only small deviations of the P3HT absorption peak at about 500nm. Since there are no obvious visible alteration of the samples' appearance and colouring (**Figure 9b**), we can assume that those absorptivity deviations may be due to difficulties in the positioning of the quite thick glass substrate in the DRS device.

**Table 2:** Reaction conditions and images of the produced *rr*-P3HT-5F-TiO<sub>2</sub> sensitized photoanodes.

| a/a | Concentration <i>rr</i> -P3HT-5F/solvent | Solvent                       | Reaction time (h) | <i>rr</i> -P3HT-5F-TiO <sub>2</sub> photoanodes                                     |
|-----|--|-------------------------------|-------------------|---|
| 1   | 5mg/5mL                                  | acetone                       | 96                |   |
| 2   | 20mg/5mL                                 | acetone                       | 96                |  |
| 3   | 20mg/4mL                                 | NMP                           | 72                |  |
| 4   | 20mg/5mL                                 | cyclohexanone / acetone (1/1) | 72                |  |
| 5   | 15mg/3mL                                 | acetone                       | 48                |  |
| 6   | 15mg/3mL                                 | acetone                       | 48                |  |
| 7   | 15mg/3mL                                 | acetone                       | 48                |  |

### Performance of DSSCs

DSSCs have been constructed as explained in the Experimental section and they have been characterized in terms of their

current-voltage characteristics. **Figure 10** shows data obtained with two sensitized photoanodes *rr*-P3HT-5F-TiO<sub>2</sub>/FTO entry 6 and entry 4 of **Table 2**. The most efficient sensitization was obtained from the conditions employed in entry 6 of **Table 2**, while entry 4 gave a poor performance, both in terms of current and voltage but also in terms of the total efficiency, as seen by the data extracted from **Figure 10** which are listed in **Table 3**. The currents obtained with the present sensitizer are much smaller than can be reached by the standard Ru-complex sensitizers.<sup>47</sup> Of course, the present data are not yet optimized. However, they suffice to show the feasibility of the presently proposed anchoring procedure on nanoparticulate titania.

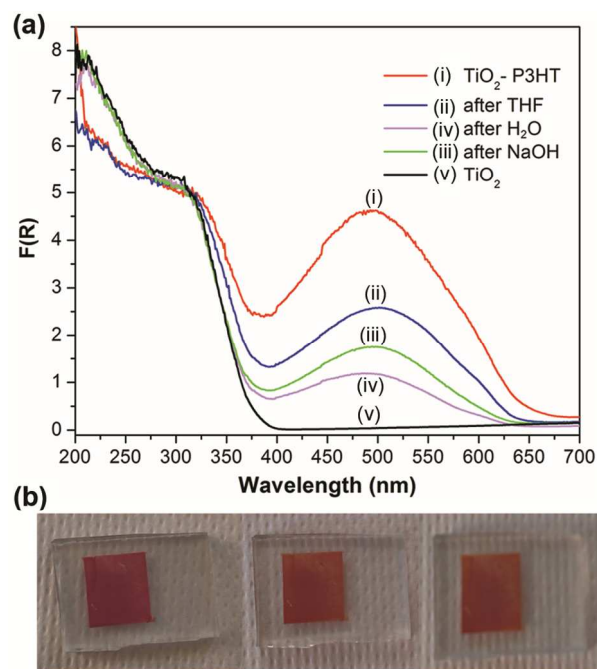


**Figure 9:** Normalized UV-Vis diffuse reflectance spectra of *rr*-P3HT-5F-TiO<sub>2</sub> photoanode (entry 7) after their subsequent immersion in THF, water and aqueous NaOH 2M solutions. The images below were taken after each solution treatment, respectively.

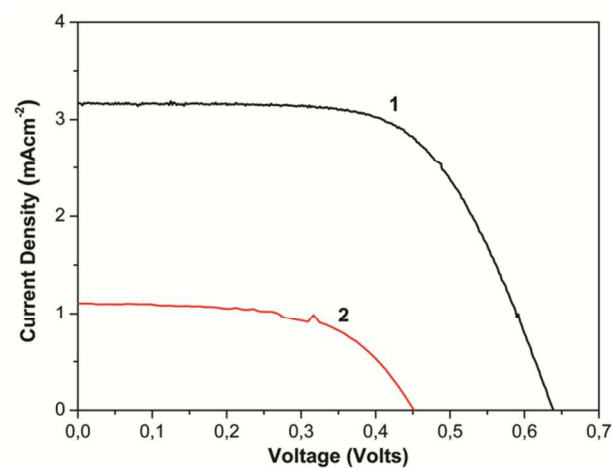


**Figure 10.** JV curves recorded with DSSC cells made by using *rr*-P3HT-5F-TiO<sub>2</sub>/FTO photoanodes: (1) entry 6 and (2) entry 4 from **Table 2**.

**Table 3.** DSSC current-voltage characteristics extracted from **Figure 10**, using the photoanodes entry 6 and entry 4 of **Table 2**.

| Type of Photoanode                                | Voc (Volts) | Jsc (mA.cm <sup>-2</sup> ) | FF   | η    |
|---|-------------|----------------------------|------|------|
| <i>rr</i> -P3HT-5F-TiO <sub>2</sub> (entry 6)/FTO | 0.64        | 3.17                       | 0.63 | 1.27 |
| <i>rr</i> -P3HT-5F-TiO <sub>2</sub> (entry 4)/FTO | 0.45        | 1.1                        | 0.62 | 0.31 |

### Study of photoelectrochemical cells

In the present work, we used a standard photoelectrochemical cell in a 2-electrode configuration employing a sensitized nc-TiO<sub>2</sub> photoanode and a counter electrode made of carbon cloth bearing a Pt/carbon-black electrocatalyst, as explained in the Experimental section. Both electrodes were in contact with an aqueous alkaline electrolyte. When the photoanode is illuminated by UV or solar light, electron-hole pairs are generated. Electrons move through an external load to the counter electrode and carry out reduction reactions. In the present case, oxygen is reduced according to the reaction<sup>59</sup>:  $\text{H}_2\text{O} + \frac{1}{2} \text{O}_2 + 2\text{e}^- \rightarrow 2\text{OH}^-$ . Holes are consumed by oxidation reactions, i.e. by water oxidation in the present case. In **Figure 11**, the efficiency of the above process is reflected into the current produced. Negligible current was produced in the dark but substantial current was produced in the case of bare nc-TiO<sub>2</sub> photoanode. The open-circuit voltage in that case reached about 1 V. In the presence of the *rr*-P3HT-5F sensitizer, a further increase of the current was observed suggesting a modest sensitization by the anchored dye. The open-circuit voltage did not change. This is an indication of sensitization. Excited dye ejects its excited electron into the conduction band of the majority species, i.e. nc-TiO<sub>2</sub>, which defines the voltage. The above data were preserved under several hours of illumination, indicating a stable photoanode. Increased current in the presence of the anchored dye may derive from dye oxidation, consumption of holes and liberation of more electrons. Such dye consumption was not presently observed, as controlled by UV-vis spectrophotometry. Even though, the above data are preliminary and further studies are necessary, they do indicate that the above dye, anchored on nc-TiO<sub>2</sub> under the present procedures, can be used as sensitizer in an aqueous alkaline environment.

### Conclusions

We have developed a novel and efficient methodology for the sensitization of TiO<sub>2</sub> nanoparticles and electrodes with organic semiconducting dyes namely small molecular quinolines and most importantly regioregular poly(3-alkyl thiophene) polymeric chains. For this purpose perfluorophenyl functionalities inserted onto the desired organic dye moieties reacted under mild alkaline conditions with the hydroxyl groups of TiO<sub>2</sub> NPs. Through this route stable and non-hydrolysable Ti-O-C bonds were formed. After optimization of the reaction conditions the final hybrid semiconducting - TiO<sub>2</sub> NPs were characterized for their optoelectronic properties and for their morphology revealing the successful incorporation of the organic moieties onto TiO<sub>2</sub>. The preservation of the anatase

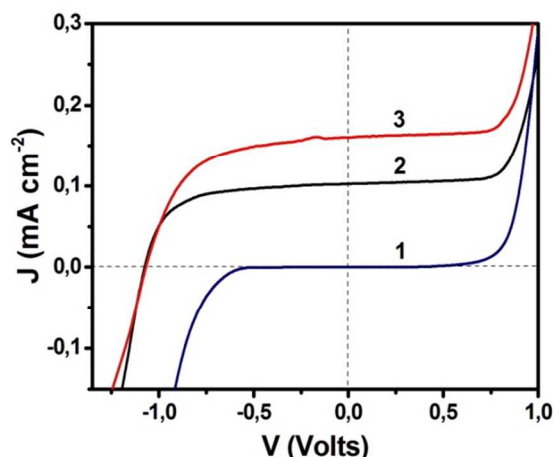


**Figure 11.** JV curves traced in a 2-electrode configuration recorded in an aqueous alkaline electrolyte containing 0.5 M NaOH and using *rr*-P3HT-5F-TiO<sub>2</sub>/FTO photoanode (same conditions as in entry 7, **Table 2**) and a Pt/CC counter electrode: (1) Curve traced in the dark; (2) bare titania without sensitizer and (3) photoanode with sensitizer.

form of TiO<sub>2</sub>, the existence of Ti-O-F bonds and the photoluminescence quenching of semiconducting moieties after their covalent attachment onto the TiO<sub>2</sub> NPs clearly demonstrate the efficacy of the particular methodology. Moreover the same conditions were employed and optimized for the sensitization of TiO<sub>2</sub> photoanodes that were tested in Dye-sensitized solar cells and in photoelectrochemical cells for water splitting under alkaline conditions. Although not yet optimized the operational features of both devices point out the viability and reliability of the proposed route.

### Acknowledgements

The authors wish to acknowledge Dr. Maria Antoniadou for the help with the photoelectrochemical measurements, Dr. Vassilios Dracopoulos for the XRD and SEM measurements and Dr. J. Vakros for his help with the UV-Vis DRS measurements.

This research has been co-financed by the European Union (European Social Fund-ESF) and Greek national funds through the Operational Program "Education and Lifelong Learning" of the National Strategic Reference Framework (NSRF)-Research Funding Program: THALES. Investing in knowledge society through the European Social Fund. Project title: "Innovative materials for nanocrystalline solar cells" (MIS: 377756).

### Notes and references

- <sup>a</sup> Department of Chemistry, University of Patras, University Campus, Rio-Patras, GR26504, Greece. Fax: +302610997122; Tel: +302610962652; E-mail: [andreopo@upatras.gr](mailto:andreopo@upatras.gr).
- <sup>b</sup> Foundation for Research and Technology Hellas / Institute of Chemical Engineering Sciences (FORTH/ICE-HT), Platani Str., Patras, GR26504, Greece
- <sup>c</sup> Department of Chemical Engineering, University of Patras, 26504 Patras, Greece.
- <sup>1</sup>Q. Schiermeier, J. Tollefson, T. Scully, A. Witze and O. Morton, *Nature*, 2008, **454**, 816-823 (DOI:10.1038/454816a).
- <sup>2</sup>J. Roncali, *Acc. Chem. Res.*, 2009, **42**, 1719-1730 (DOI: 10.1021/ar900041b).

- <sup>3</sup>G. Dennler, M. C. Scharber and C. J. Brabec, *Adv. Mater.*, 2009, **21**, 1323-1338 (DOI:10.1002/adma.200801283).
- <sup>4</sup>J. Chen and Y. Cao, *Acc. Chem. Res.*, 2009, **42**, 1709-1718 (DOI: 10.1021/ar900061z).
- <sup>5</sup>B. Bozic-Weber, E. C. Constable and C. E. Housecroft, *Coord. Chem. Rev.*, 2013, **257**, 3089-3106 (DOI: 10.1016/j.ccr.2013.05.019).
- <sup>6</sup>H. M. Upadhyaya, S. Senthilarasu, M.-H. Hsu and D. K. Kumar, *Sol. Energy Mater. Sol. Cells*, 2013, **119**, 291-295 (DOI: 10.1016/j.solmat.2013.08.031).
- <sup>7</sup>B. O'Regan and M. Grätzel, *Nature*, 1991, **353**, 737-740 (DOI:10.1038/353737a0).
- <sup>8</sup>J. Bouclé and J. Ackermann, *Polym. Int.*, 2012, **61**, 355-373 (DOI:10.1002/pi.3157).
- <sup>9</sup>J. Qu and C. Lai, *J. Nanomater.* 2013, **2013**, Article ID 762730, 11 pages (DOI:10.1155/2013/762730).
- <sup>10</sup>H. C. Weerasinghe, F. Huang and Y.-B. Cheng, *Nano Energy*, 2013, **2**, 174-189 (DOI: 10.1016/j.nanoen.2012.10.004).
- <sup>11</sup>Q. Zhang, C. S. Dandeneau, X. Zhou and G. Cao, *Adv. Mater.*, 2009, **21**, 4087-4108 (DOI:10.1002/adma.200803827).
- <sup>12</sup>A. L. Brisenio, T. W. Holcombe, A. I. Boukai, E. C. Garnett, S. W. Shelton, J. J. M. Fréchet and P. Yang, *Nano Lett.*, 2010, **10**, 334-340 (DOI: 10.1021/nl9036752).
- <sup>13</sup>B. Onwona-Agyeman, S. Kaneko, A. Kumara, M. Okuya, K. Murakami, A. Konno and K. Tennakone, *Jpn. J. Appl. Phys.*, 2005, **44**, 731-733 (DOI:10.1143/JJAP.44.L731).
- <sup>14</sup>Y.-F. Wang, J.-W. Li, Y.-F. Hou, X.-Y. Yu, C.-Y. S. Prof. and D.-B. K. Prof., *Chem. Eur. J.*, 2010, **16**, 8620-8635 (DOI: 10.1002/chem.201001333).
- <sup>15</sup>L. Cojocaru, C. Olivier, T. Toupance, E. Sellier and L. Hirsch, *J. Mater. Chem. A*, 2013, **1**, 13789-13799 (DOI: 10.1039/C3TA12279D).
- <sup>16</sup>A. Hagfeldt, G. Boschloo, L. Sun, L. Kloo and H. Pettersson, *Chem. Rev.*, 2010, **110**, 6595-6663 (DOI: 10.1021/cr900356p).
- <sup>17</sup>M. K. Nazeeruddin, A. Kay, I. Rodicio, R. Humphry-Baker, E. Mueller, P. Liska, N. Vlachopoulos and M. Graetzel, *J. Am. Chem. Soc.*, 1993, **115**, 6382-6390 (DOI: 10.1021/ja00067a063).
- <sup>18</sup>T. Funaki, N. Onozawa-Komatsuzakia, K. Kasugab, K. Sayama and H. Sugihara, *Inorg. Chem. Commun.*, 2013, **35**, 281-283 (DOI: 10.1016/j.inoche.2013.06.047).
- <sup>19</sup>T. Funaki, H. Kusama, N. Onozawa-Komatsuzaki, K. Kasuga, K. Sayama and H. Sugihara, *Eur. J. Inorg. Chem.*, 2014, **2014**, 1303-1311 (DOI: 10.1002/ejic.201301459).
- <sup>20</sup>T. Bessho, E. C. Constable, M. Graetzel, A. Hernandez Redondo, C. E. Housecroft, W. Kylberg, M. K. Nazeeruddin, M. Neuburger and S. Schaffner, *Chem. Commun.*, 2008, **32**, 3717-3719 (DOI: 10.1039/B808491B).
- <sup>21</sup>K. A. Wills, H. J. Mandujano-Ramírez, G. Merino, D. Mattia, T. Hewat, N. Robertson, G. Oskam, M. D. Jones, S. E. Lewis and P. J. Cameron, *RSC Adv.*, 2013, **3**, 23361-23369 (DOI: 10.1039/C3RA44936J).
- <sup>22</sup>D. Kuciauskas, J. E. Monat, R. Villahermosa, H. B. Gray, N. S. Lewis and J. K. McCusker, *J. Phys. Chem. B*, 2002, **106**, 9347-9358 (DOI: 10.1021/jp014589f).
- <sup>23</sup>S. Altobello, R. Argazzi, S. Caramori, C. Contado, S. Da Fré, P. Rubino, C. Choné, G. Larramona and C. A. Bignozzi, *J. Am. Chem. Soc.*, 2005, **127**, 15342-15343 (DOI: 10.1021/ja053438d).
- <sup>24</sup>S. Ferrere and B. A. Gregg, *J. Am. Chem. Soc.*, 1998, **120**, 843-844 (DOI: 10.1021/ja973504e).
- <sup>25</sup>S. Ferrere, *Inorg. Chim. Acta*, 2002, **329**, 79-92, (DOI: 10.1016/S0020-1693(01)00743-5).
- <sup>26</sup>J. Fujimoto, K. Manseki and H. Miyaji, *Chem. Lett.*, 2014, **43**, 207-209 (DOI:10.1246/cl.130880).
- <sup>27</sup>A. Irfan, N. Hina, A. G. Al-Sehemi and A. M. Asiri, *J. Mol. Model.*, 2012, **18**, 4199-4207 (DOI: 10.1007/s00894-012-1421-4).
- <sup>28</sup>D. K. Panda, F. S. Goodson, S. Raya and S. Saha, *Chem. Commun.*, 2014, **50**, 5358-5360 (DOI: 10.1039/C3CC47498D).
- <sup>29</sup>M.-E. Ragoussi, J.-H. Yum, A. K. Chandiran, M. Ince, G. de la Torre, M. Grätzel, M. K. Nazeeruddin and T. Torres, *Chem. Phys. Chem.*, 2014, **15**, 1033-1036 (DOI:10.1002/cphc.201301118).
- <sup>30</sup>P. Gao, H. N. Tsao, C. Yi, M. Grätzel and M. K. Nazeeruddin, *Adv. Energy Mater.*, 2014, **4**, 1301485 (DOI: 10.1002/aenm.201301485).
- <sup>31</sup>D. Joly, L. Pellejà, S. Narbey, F. Oswald, J. Chiron, J. N. Clifford, E. Palomares and R. Demadrille, *Sci. Rep.*, 2014, **4**, Article number 4033 (DOI:10.1038/srep04033).
- <sup>32</sup>A. Mishra, M.K.R. Fischer and P. Bäuerle, *Angew. Chem. Int. Ed.*, 2009, **48**, 2474-2499 (DOI:10.1002/anie.200804709).
- <sup>33</sup>Y.-S. Yen, H.-H. Chou, Y.-C. Chen, C.-Y. Hsu and J. T. Lin, *J. Mater. Chem.*, 2012, **22**, 8734-8747 (DOI: 10.1039/c2jm30362k).
- <sup>34</sup>L. Schmidt-Mende, U. Bach, R. Humphry-Baker, T. Horiuchi, H. Miura, S. Ito, S. Uchida and M. Grätzel, *Adv. Mater.*, 2005, **17**, 813-815 (DOI:10.1002/adma.200401410).
- <sup>35</sup>M. Antoniadou, E. Stathatos, N. Boukos, A. Stefopoulos, J. Kallitsis, F. C. Krebs and P. Lianos, *Nanotechnology*, 2009, **20**, 495201 (9pp) (DOI:10.1088/0957-4484/20/49/495201).
- <sup>36</sup>F. Boon, A. Thomas, G. Clavel, D. Moerman, J. De Winter, D. Laurencin, O. Coulembier, P. Dubois, P. Gerbaux, R. Lazzaroni, S. Richeter, A. Mehdi and S. Clément, *Synthetic Met.*, 2012, **162**, 1615-1622 (DOI: 10.1016/j.synthmet.2012.07.026).
- <sup>37</sup>R. A. Kruger, T. J. Gordon, T. Baumgartner and T. C. Sutherland, *ACS Appl. Mater. Interfaces*, 2011, **3**, 2031-2041 (DOI: 10.1021/am200262w).
- <sup>38</sup>S. Ardo and G. J. Meyer, *Chem. Soc. Rev.*, 2009, **38**, 115-164 (DOI: 10.1039/B804321N).
- <sup>39</sup>P. Péchy, F. P. Rotzinger, M. K. Nazeeruddin, O. Kohle, S. M. Zakeeruddin, R. Humphry-Baker and M. Grätzel, *J. Chem. Soc., Chem. Commun.*, 1995, 65-66 (DOI: 10.1039/C39950000065).
- <sup>40</sup>C. Baik, D. Kim, M.-S. Kang, S. O. Kang, J. Ko, M. K. Nazeeruddin and M. Grätzel, *J. Photochem. Photobiol., A*, 2009, **201**, 168-174 (DOI: 10.1016/j.jphotochem.2008.10.018).
- <sup>41</sup>C. Koenigsmann, T. S. Ripolles, B. J. Brennan, C. F. A. Negre, M. Koepf, A. C. Durrell, R. L. Milot, J. A. Torre, R. H. Crabtree, V. S. Batista, G. W. Brudvig, J. Bisquert and C. A. Schmuttenmaer, *Phys. Chem. Chem. Phys.*, 2014, **16**, 16629-16641 (DOI: 10.1039/C4CP02405B).
- <sup>42</sup>T. P. Brewster, S. J. Konezny, S. W. Sheehan, L. A. Martini, C. A. Schmuttenmaer, V. S. Batista and R. H. Crabtree, *Inorg. Chem.*, 2013, **52**, 6752-6764 (DOI: 10.1021/ic4010856).
- <sup>43</sup>R. S. Loewe, P. C. Ewbank, J. Liu, L. Zhai and R. D. McCullough, *Macromolecules*, 2001, **34**, 4324-4333 (DOI: 10.1021/ma001677+).
- <sup>44</sup>S. Kakogianni, S. N. Kourkoulis, A. K. Andreopoulou and J. K. Kallitsis, *J. Mater. Chem. A*, 2014, **2**, 8110-8117 (DOI: 10.1039/C4TA00741G).
- <sup>45</sup>M.-I. Baraton and L. Merhari, *J. Eur. Ceram. Soc.*, 2004, **24**, 1399-1404 (DOI: 10.1016/S0955-2219(03)00419-9).
- <sup>46</sup>A. Nikolakopoulou, D. Tasis, L. Sygellou and P. Lianos, *Electrochim. Acta*, 2014, **139**, 54-60 (DOI: 10.1016/j.electacta.2014.06.154).
- <sup>47</sup>A. Nikolakopoulou, D. Tasis, L. Sygellou, V. Dracopoulos, C. Galiotis and P. Lianos, *Electrochim. Acta*, 2013, **111**, 698-706 (DOI: 10.1016/j.electacta.2014.06.154).
- <sup>48</sup>E. Stathatos, P. Lianos, U.L. Stangar, B. Orel and P. Judeinstein, *Langmuir*, 2000, **16**, 8672-8676 (DOI: 10.1021/la0002987).
- <sup>49</sup>M. Antoniadou, S. Sfaelou and P. Lianos, *Chem. Eng. J.*, 2014, **254**, 245-251 (DOI: 10.1016/j.cej.2014.05.106).
- <sup>50</sup>A. A. Stefopoulos, S. N. Kourkoulis, S. Economopoulos, F. Ravani, A. Andreopoulou, K. Papagelis, A. Siokou and J. K. Kallitsis, *Macromolecules* 2010, **43**, 4827-4828 (DOI: 10.1021/ma100961y).
- <sup>51</sup>X. Wang, S. Meng, X. Zhang, H. Wang, W. Zhong and Q. Du, *Chem. Phys. Lett.*, 2007, **444**, 292-296 (DOI: 10.1016/j.cplett.2007.07.026).
- <sup>52</sup>Y. Lee, M. Kang, *Materials Chemistry and Physics* 2010, **122**, 284-289 (DOI: 10.1016/j.matchemphys.2010.02.050).
- <sup>53</sup>R. Urlaub, U. Posset, R. Thull, *Journal of Non-Crystalline Solids* 2000, **265**, 276-284 (DOI: 10.1016/S0022-3093(00)00003-X).
- <sup>54</sup>F. N. Castellano, J. M. Stipkala, L. A. Friedman, G. J. Meyer, *Chem. Mater.* 1994, **6**, 2123-2129 (DOI: 10.1021/cm00047a037).
- <sup>55</sup>M. Karabacak, E. Kose and M. Kurt, *J. Raman Spectrosc.* 2010, **41**, 1085-1097 (DOI 10.1002/jrs.2551).

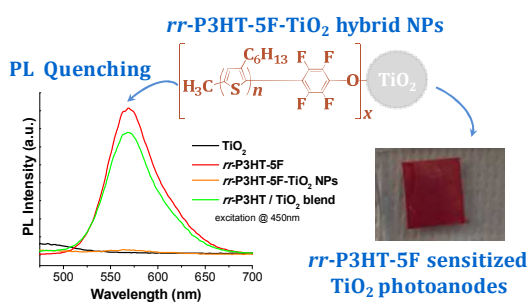
- 
- <sup>56</sup>A. A. Stefopoulos, C. L. Chochos, M. Prato, G. Pistolis, K. Papagelis, F. Petraki, S. Kennou and J. K. Kallitsis, *Chem. Eur. J.* 2008, **14**, 8715-8724 (DOI: 10.1002/chem.200800683).
- <sup>57</sup>M. Konstantakou, T. Stergiopoulos, V. Likodimos, G. C. Vougioukalakis, L. Sygellou, A. G. Kontos, A. Tserepi and P. Falaras, *J. Phys. Chem. C*, article in press (DOI: 10.1021/jp412766f).
- <sup>58</sup>P. Dannetun, M. Boman, S. Stafström C. Fredriksson, J. L. Bredas, R. Zamboni, C. Taliani and W. R. Salaneck, *J. Chem. Phys.*, 1993, **99**, 664 (DOI: 10.1063/1.466217).
- <sup>59</sup>P. Lianos, *Journal of Hazardous Materials*, 2011, **185**, 575-590 (DOI: 10.1016/j.jhazmat.2010.10.083).

# An alternative anchoring methodology of organic sensitizers onto TiO<sub>2</sub> semiconductors for photoelectrochemical applications

5 Panagiotis Giannopoulos,<sup>a,b</sup> Archontoula Nikolakopoulou,<sup>b,c</sup> Aikaterini K. Andreopoulou,<sup>\*a,b</sup> Lamprini Sygellou,<sup>b</sup> Joannis K. Kallitsis,<sup>a,b</sup> and Panagiotis Lianos<sup>b,c</sup>

## Table of Contents entry

10 Perfluorophenyl functionalized organic semiconducting dyes have been employed for the development of TiO<sub>2</sub> organic hybrid NPs via stable non-hydrolysable Ti-O-C bonds. Photoanodes prepared thereof were tested in DSSCs and photoelectrochemical cells.



15